ACS ORGANIC & INORGANIC Au
AN OPEN ACCESS JOURNAL OF THE AMERICAN CHEMICAL SOCIETY

pubs.acs.org/orginorgau

Review

Roles of Metal Ions in Foldamers and Other Conformationally Flexible Supramolecular Systems

Jess L. Algar, James A. Findlay, and Dan Preston*

Cite This: ACS Org. Inorg. Au 2022, 2, 464−476

Read Online

ACCESS | Metrics & More | Article Recommendations

ABSTRACT: Conformational control is a key prerequisite for much molecular function. As chemists seek to create complex molecules that have applications beyond the academic laboratory, correct spatial positioning is critical. This is particularly true of flexible systems. Conformationally flexible molecules show potential because they resemble in many cases naturally occurring analogues such as the secondary structures found in proteins and peptides such as α-helices and β-sheets. One of the ways in which conformation can be controlled in these molecules is through interaction with or coordination to metal ions. This review explores how secondary structure (i.e., controlled local conformation) in foldamers and other conformationally flexible systems can be enforced or modified through coordination to metal ions. We hope to provide examples that illustrate the power of metal ions to influence this structure toward multiple different outcomes.

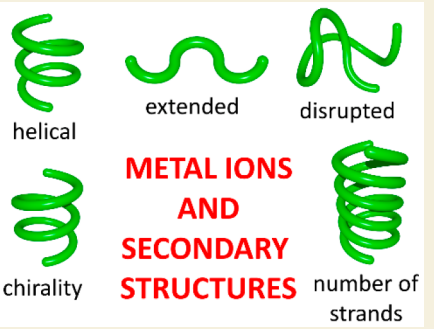

KEYWORDS: *conformation, metallofoldamers, foldamers, self-assembly, supramolecular, metal ions, flexibility, metallo-supramolecular, secondary structure*

1. INTRODUCTION

In metallo-supramolecular systems, structure is defined through the combination of connectivity and conformation. The role of the metal ion in connectivity is self-evident in the formation of coordination bonds. However, the role of metal ions in conformation is not so straightforward and requires consideration of the particular system at hand.

These systems can be considered from the vantage point of the flexibility (or lack thereof) of the ligands. In many cases, metallo-supramolecular systems are built from rigid ligands with limited degrees of freedom, and it is this rigidity that defines the three-dimensional structure. The classic example of this sort is coordination cages, also known as metal−organic cages.[1−3] In this respect, conformational control is greatly enabled by the cyclic nature of these structures.

There are also systems built around ligands with far greater flexibility. In some of these, metal ions are critical for conformational control. The systems we will discuss include examples of foldamers, and other conformationally flexible systems. Foldamers, as defined by Moore and co-workers,[4] are single- or multiple-stranded oligomers that fold into conformationally ordered states in solution due to supramolecular interactions. The interactions that have been utilized in this manner include hydrogen,[5,6] halogen,[7,8] or chalcogen bonds[9] and $\pi-\pi$ interactions,[10−12] solvent effects,[13−15] or combinations thereof, in addition to the coordination bond that will be discussed here. Foldameric structures have been targeted for applications including the guest binding of anions[16−20] and other molecules,[21−23] catalysis,[24−28] ion,[29−31] or charge transport,[32] and electron transfer.[33]

Foldamers have been well reviewed.[4,34−39] With respect to metallofoldamers, there is a book from 2013 giving comprehensive background to the area,[40] a 2009 review from Maayan which breaks down metallofoldamers by the structural role the metal ion plays,[41] and a recent 2021 review on metal-binding foldamers.[42] There are other reviews on the roles that metal ions can play in proteins and peptides.[43,44]

We hope to bring a fresh perspective here, with a review of the literature with respect to the influence that the metal ion has upon the secondary structure or conformation of foldamers or other conformationally flexible systems. Just as with naturally occurring secondary structure analogues such as α-helices and β-sheets in peptides and proteins, it is conformational control that enables potential function. As such, understanding the roles that metal ions can play in the conformation of flexible systems is crucial. Most examples given in previous reviews focus upon coordination of a (often previously amorphous) foldamer strand to a metal ion, giving a helical conformation. For completeness, we include some

Received: May 9, 2022
Revised: August 4, 2022
Accepted: August 8, 2022
Published: August 22, 2022

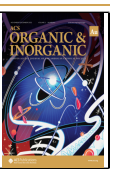

https://doi.org/10.1021/acsorginorgau.2c00021
ACS Org. Inorg. Au 2022, 2, 464−476

examples of this sort, but our main focus are other ways that metal ions can contribute to conformational control, such as the formation of other structural types such as extended structures or turns or the alteration of helix properties such as pitch, stability, handedness and single-to-double helix conversion. We also include some examples of coordination complexes, where we think they aid the consideration of the ways that metal ions can contribute to conformation in flexible systems.

2. METAL IONS PROMOTING THE FORMATION OF HELICES

Before the formation of a secondary foldamer structure through the addition of the metal ion(s), the primary organic sequence can exist either in an amorphous state or in another ordered state which is converted into a helix. Hence, metalation can either create order where before there was none or act as a stimulus for the transformation from one ordered secondary structure to another.

2.1. From Ill-Defined Conformations to Helices

The most common way in which the combination of metal ions to a flexible ligand results in helix formation has been to coordinate to the strand, providing rigidification. This is often accompanied by additional stabilization through solvophobic effects/$\pi-\pi$ interactions[45] or hydrogen bonding.[46] Akine, Nabeshima, and co-workers have also utilized the incorporation of metal ions into salen-type complexes to enforce helicity on multiple occasions.[47−50] Their general strategy has been to use ligands with multiple salen sites in combination with multiple Zn(II) ions, which due to the incorporation of chiral groups, lead to formation of single-handed helices. These metallofoldamers can then bind lanthanides, with the capacity to invert helicity often endowed through exchange of lanthanides of different size. In other work using salen-type complexes, Tanaka and co-workers have recently combined the use of metal ions coordinating to strands with integration of metal ions into the foldamer backbone.[51] They have reported a system utilizing a bis-β-diketonate ligand with a central salen core. Both Ni(II) and Pd(II) could be coordinated to the salen group. They were then able to combine this metalloligand in 2:1 stoichiometry with Pd(II) through coordination to one of the diketonate groups, integrating the metal ion into the backbone. The resultant complexes were mesogenic and demonstrated thermotropic columnar liquid crystallinity.

Metal binding does not have to be confined to integration within the backbone, or *endo* coordination to heteroatoms that make up the backbone. It has also been demonstrated to be possible at side chain sites. Maayan and co-workers have synthesized peptoid oligomers with four metal binding chelators as side chains: either four 8-hydroxyquinoline (HQ) units or a 3:1 HQ/terpyridine ratio. The peptoids were unstructured in the absence of metal ions but adopted helical structures when metal ions were added. Most notably, positive allostery between different metal ions was demonstrated. Cu(II) bound preferentially in a HQ+terpy site, inducing folding that facilitated coordination of another metal ion (Zn(II) or Co(II)) in the remaining HQ+HQ site.[52] The metal/ligand ratios for these complexes (and other similar peptoid complexes discussed in this review) were established through UV spectroscopic titrations.

However, our focus in this section is where metal ions are integrated into the primary structure of the molecule (i.e., in the molecular backbone) and contribute to secondary structure in other ways, namely, through metallophillic interactions or through influencing the electronic character of the molecule for $\pi-\pi$ interactions. For example, metal ions have also been introduced as capping units for foldamers by Yam and co-workers.[53,54] They reported six different bisacetylide ligands which were linked by five six-membered aromatic rings, in turn, joined by acetylene units (**L1**, Figure 1). The identity of the aromatic rings varied between pyridine and phenyl groups; for example, Ph−Ph−Py−Ph−Ph consists only of phenyl rings except for a central pyridine. The acetylides were coordinated to Pt(terpy) units to give $[(Pt(terpy)_2)_2\mathbf{L1}]^{2+}$ complexes. These complexes coiled into foldameric helices in acetonitrile. This coiling was driven through favorable Pt(II)−Pt(II) interactions: the metallophillic interactions therefore provided the impetus for the formation of secondary structure, as well as $\pi-\pi$ interactions between the Pt(II) coordinative environments. Clear evidence of coiling was given through ^{1}H ROESY NMR spectroscopy and UV−visible spectroscopy. These interactions (and hence the formation of the foldamer) could be disrupted by increasing the ratio of dichloromethane to acetonitrile, by increasing temperature, and by addition of acid which protonates the pyridine units in the ligand backbone. Reversal of these stimuli resulted in reformation of the foldamer (Figure 1). The same group has used similar poly(ethynylbenzene) foldamers with 2,6-bis(*N*-dodecylbenzimidazol-2′-yl)pyridine tridentate capping ligands which form metallogels using the same interactions as in the previous example.[55]

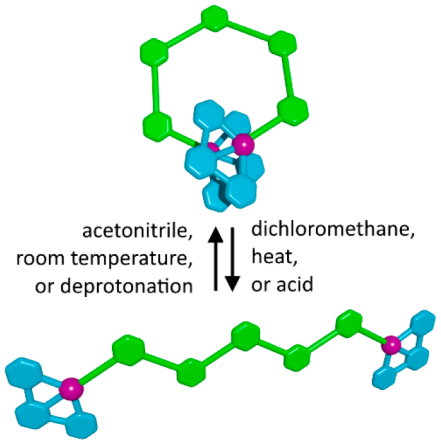

Figure 1. $[(Pt(terpy))_2\mathbf{L1})]^{2+}$ complexes used by Yam and co-workers,[54] in which helical formation was driven by metallophilic interactions: coiling/uncoiling could be influenced by solvent, temperature, or pH.

Preston recently reported a system in which discrete heteroleptic systems can be assembled with hemilabile Pd(II).[56] The controllable formation of heteroleptic metal coordination environments was achieved through the use of various pairs of ligand sites that were complementary to one another with respect to square planar metal ions. This complementarity was driven by denticity (3:1 tridentate and monodentate and 2:2 bis-bidentate, Figure 2) and/or by complementary intraligand hydrogen-bonding arrays. Bidentate chelators had either two hydrogen bond acceptor sites or two hydrogen bond donor sites (complementary to one another, 2:2′) or one hydrogen bond acceptor site and one

https://doi.org/10.1021/acsorginorgau.2c00021
ACS Org. Inorg. Au 2022, 2, 464−476

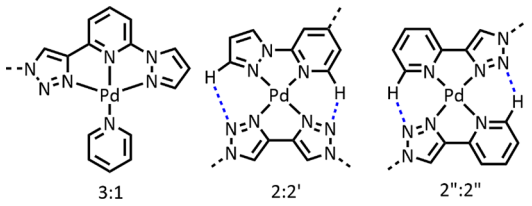

Figure 2. Complementary pairings used by Preston to integrate metal ions into the primary structure of heteroleptic metallofoldamers.[56] Left, 3:1 complementarity; center, 2:2′ complementarity; right, 2′′:2′′ complementarity. Hydrogen bonds are shown with blue dotted lines.

hydrogen bond donor site (self-complementarity, 2″:2″). Using ligands with different combinations of these sites, discrete heteroleptic sequences with Pd(II) junctions were obtained.

While the palladium(II) metal ions were instrumental in forming the foldamer backbone, they were also involved in defining helical conformation through $\pi-\pi$ interactions. The ligands possessed electron-rich anthracene units, with high affinity for the electron-deficient aromatic areas in the coordinative environments of the sequences formed. This promoted coiling of the complexes (Figure 3). Conformational information about the foldamers was obtained by a combination of 2D NMR spectroscopies, molecular dynamics simulations, and, in one case, crystallography.

2.2. From Extended Conformations to Helices

Rather than forming foldamers from ligands that are poorly structurally defined in the absence of metal ions, others have used metal ions to switch from one secondary structural type to another. This requires a driving force that imparts controllable and converse structure to both the metalated and nonmetalated forms. This has been accomplished through the use of sites with the potential to bind metal ions that adopt opposite conformations depending on whether or not metal coordination is occurring. These sites have been termed "structural codons" by Lehn and co-workers,[57] and the driving force for reversal of conformation has been intramolecular hydrogen bonding (Figure 4). The noncoordinated ligand conforms to maximize hydrogen bonding between nitrogen atoms and hydrogen atoms in adjacent positions, hence nitrogen atoms are orientated *anti* to one another. Upon coordination, there is a rotation around these bonds giving a *syn* conformation. A large number of structural codons have been employed to these ends, including terpy (pyridine−pyridine−pyridine), pyridine−hydrazone−pyridine, hydrazone−triazine−hydrazone, and many others.

Depending on the substitution pattern surrounding the codon, the secondary structure is driven from an extended form to a helical form either by addition or by removal of the metal ion (for example, with α,α-substituted pyridyl units) or the reverse (α,β-pyridyl units). For example, a ligand system providing a variant on this theme has been reported by Pipilier, Huc, and co-workers.[58] This ligand (**L7**) featured a diacid pyridazine−pyridine−pyridazine central codon that when nonmetalated was in the extended conformation (Figure 5). Attached to either side of this were primary sequences consisting of two amino napthyridine acid units, an amino-pyridine unit, and three aminoquinoline acid units (they also made a similar ligand with an additional pyridoquinoline unit, to similar effect).

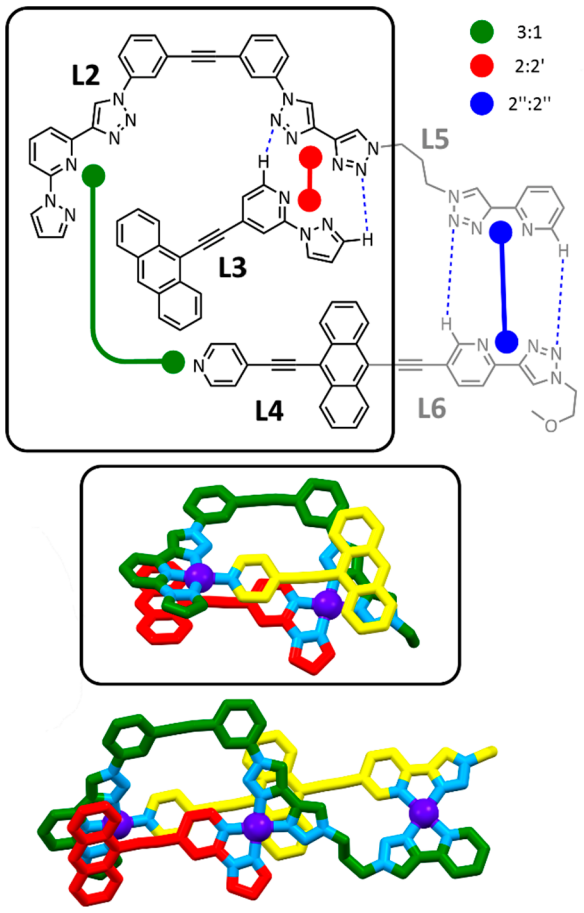

Figure 3. Construction of foldamers using orthogonal complementary pairs by Preston: ligands **L2** (ditopic), **L3** (monotopic), and **L4** (monotopic) could be combined to form a dipalladium(II) helix (shown in the insets), whereas ligands **L5** (tritopic), **L3** (monotopic), and **L6** (ditopic) could be combined to form a tripalladium(II) cyclic foldamer (other structure). Colors: carbon, green, yellow, or red; nitrogen, light blue; palladium, dark blue.

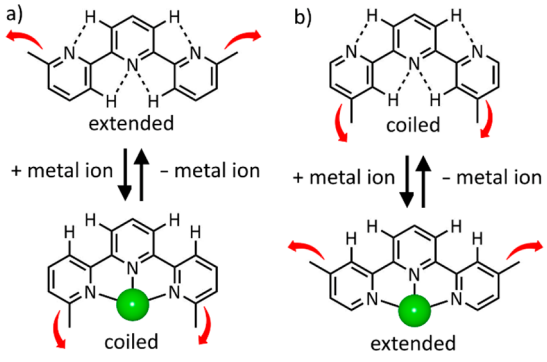

Figure 4. Structural codons that reverse their conformation between nonmetalated hydrogen-bonding modes and metal-coordinated modes, shown for a terpy system,[57] (a) metal coordination resulting in change from an extended to a coiled conformation and (b) metal coordination resulting in a change from coiled to extended conformation.

Without metal ions, the two peripheries of coiled **L7**, linked by the extended central codon into a coiled-extended-coiled secondary structure. NMR data suggested that **L7** aggregated in solution, and the molecule crystallized in **L7** dimers. Upon introduction of 1 equiv of a metal ion (either Cu(I) or Ag(I)),

https://doi.org/10.1021/acsorginorgau.2c00021
ACS Org. Inorg. Au 2022, 2, 464−476

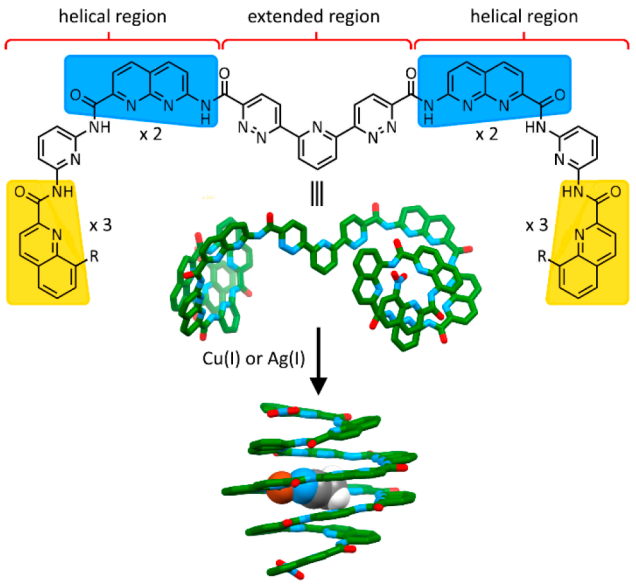

Figure 5. Poly-aza-aromatic ligand **L7** reported by Pipilier, Huc, and co-workers,[58] consisting of an extended structural codon in the center, surrounded by codons which conform to a helical shape of decreasing radius moving toward the outside (solubilizing chains omitted, R = NO_2). Areas in blue are repeated in duplicate, areas in yellow in triplicate. This results in the ligand adopting a coiled-extended-coiled structure. Upon addition of Cu(I) or Ag(I), all regions are coiled, forming a $[M\mathbf{L7}]^+$ foldameric helix. Note that the X-ray crystal structure obtained contained copper oxidized to the +2 state, in square planar geometry, with the last site on the Cu(II) ion occupied by acetonitrile (shown in space-filling view). Most hydrogen atoms and solubilizing chains are omitted for clarity. Colors: carbon, green for **L7**; acetonitrile, gray; hydrogen, white; copper, copper; nitrogen, light blue; oxygen, red.

the ^{1}H NMR spectra sharpened, due to the formation of a single coiled foldameric structure, with the metal ion in the central codon. A crystal structure was obtained for the copper complex, but with the metal ion oxidized to the +2 state (this oxidation state was not reflected in the solution-phase data). Because of the primary sequence chosen, with each structural type enforcing helical coiling on a tighter radius moving toward the outsides of the molecule, the helix was wider in the center than at the ends, creating a central cavity. An additional acetonitrile molecule was coordinated to the final site of the square planar coordination sphere of the metal ion and was encapsulated in the helical foldamer (Figure 5). This prompted the authors to investigate the solution-phase interaction between $[Cu\mathbf{L7}]^+$ and imidazole, which slowly displaced encapsulated ligated solvent within the helical structure. In subsequent work, the authors also showed helix formation upon a 1:1 introduction of alkali or alkali earth metals, with binding trends in the following order: $Ba^{2+} < K^+ \ll Ca^{2+} \approx Na^+ \ll Mg^{2+}$, with Mg^{2+} displaying higher affinity than the transition metal ions Cu(I) or Zn(II). Interestingly, the alkali and alkali earth metals displayed varying levels of retention of their waters of solvation within the cavity.[59]

Another conversion from an extended-type conformation (a double hairpin) to helical form has been achieved with square planar palladium(II) by Setsune and co-workers.[60,61] For example, they formed a hexapyrrole sequence capped with aldehydes ($H_4\mathbf{L8}$, Figure 6 top, X = O), allowing imine condensations, aided by zinc *p-tert*-butylbenzoate, to alter the terminal groups. This adopted an extended conformation due

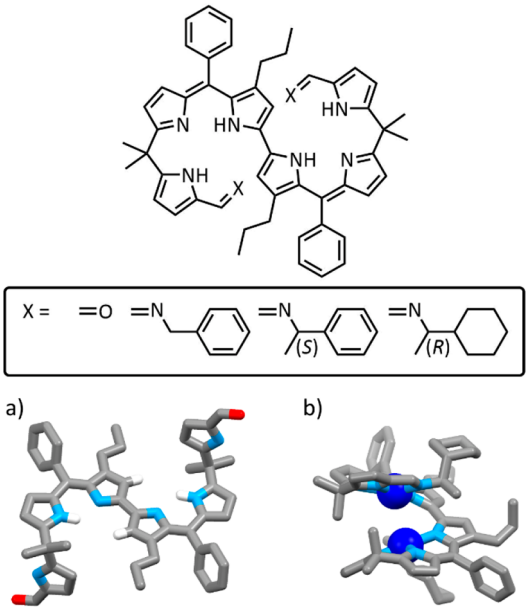

Figure 6. System reported by Setsune and co-workers[60] with (a) a (protonated) ligand (**L8**) adopting double hairpin structure and (b) conversion to a helix in the presence of Pd(II). The chirality of the X substituent influenced the isomer distribution of the products. Colors: carbon, gray; key hydrogen atoms, white; nitrogen, light blue; oxygen, red; palladium, dark blue.

to alternating NH−H hydrogen bonds between pyrrole groups (Figure 6a). Introduction of $[Pd(CH_3CN)_2Cl_2]$ to $H_4\mathbf{L8}$ in a dichloromethane/methanol solution resulted in the formation of a $[Pd_2(\mathbf{L8})]^{2+}$ foldamer that coiled helically, with each Pd(II) metal ion coordinated to three pyrrole groups and the aldehyde. They were able to carry out an additional imine condensation in situ and convert the **L8** aldehyde to a benzyl, (*S*)-1-methylbenzene or (*R*)-1-methylcyclohexane imine group (inset and Figure 6b). A preference for a particular helix enantiomer was established depending on the isomerism of some of the head groups: *S* leading to the *M* isomer and *R* leading to the *P* isomer. Osuka and co-workers reported similar dinuclear helices from Cu(II) and heptapyrroles, as well as a cyclic dicopper(II) octapyrrole lemniscate complex.[62] Likewise, Akine, Nabeshima, and co-workers reported dinuclear systems from polypyridyl ligands that convert from extended conformations to helices upon metal complexation. Intrinsic ligand chirality was also achieved through incorporation of BINOL.[63]

2.3. Distranded Helices

The popularity of pyrroles has also been seen in work from Dolphin and co-workers, with bis(dipyrromethene) ligands in which the two bidentate chelators were separated by linkers of 0, 1, or 2 carbons.[64] Combination of the ligands with Zn(II) or Co(II) in chloroform/methanol gave double-stranded $[M_2L_2]$ helices, with key $\pi-\pi$ interactions between regions of the ligand backbones. The contribution of $\pi-\pi$ interactions to the folding of poly-stranded metallohelices has subsequently been well explored by the Maayan group, using peptoid ligands in combination with Cu(II).[65] The peptoids possessed a 2,2′-bipyridine unit as one bidentate chelator, with another chelator being formed from a secondary amine and nearby amide carbonyl oxygen (Figure 7a). Identities varied in the series in two key positions. R_1 was a polar terminal group to an ethyl

https://doi.org/10.1021/acsorginorgau.2c00021
ACS Org. Inorg. Au 2022, 2, 464−476

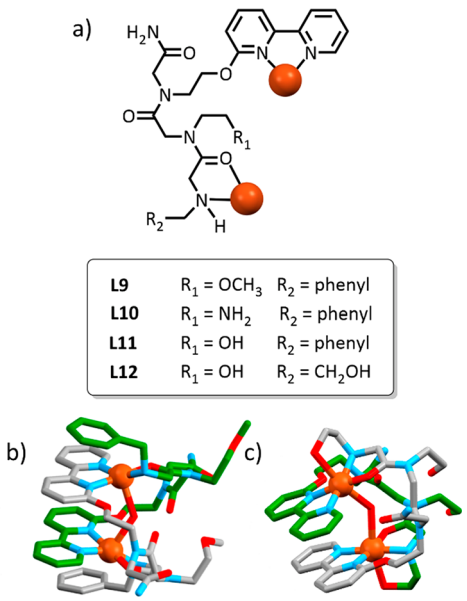

Figure 7. Double-stranded peptoid-based foldamers from Maayan and co-workers:[65] (a) core structure of peptoid ligands, showing the two bidentate sites coordinated to Cu(II), with depictions of the crystal structures of (b) $[Cu_2\mathbf{L9}_2(H_2O)](ClO_4)_4$ and (c) $[Cu_2\mathbf{L12}_2(H_2O)](ClO_4)_4$. Colors: carbon, green or gray; copper, copper; nitrogen, light blue; oxygen, red. Hydrogen atoms, solvent, and counterions are omitted for clarity.

side chain (either $-OCH_3$, $-NH_2$, or $-OH$). R_2 was the substituent off the terminal amino group making up one of the donor atoms in the secondary chelator, giving either benzyl or ethanol substitution.

With each of the three possible benzyl-containing ligands (**L9**–**L12**), the combination with Cu(II) gave 2:2 complexes.[65] While solution-phase data suggested fluxionality, the complexes crystallized with the metal ions in pentacoordinate environments. The benzyl groups were able to π-stack with the coordinating bipyridines, which also in two cases sat over each other. The identity of the fifth donor atom aside from the four from the two chelating groups depended on the nature of R_1. For the alcohol group (**L11**), this side chain was coordinated as the alkoxide, but for methoxy (**L9**) and amino (**L10**), a water molecule bridging the Cu(II) centers was coordinated (Figure 7b).

In these examples, the benzyl group also served to potentially block access to the metal ion from the outside, but different substitutions in this position could directly target coordination. As well as demonstrating that an appended pyridine could occupy the fifth coordinative site of the Cu(II) metal ions,[66] Maayan and co-workers also used the **L12** variant with R_1 and R_2 both terminating in OH groups.[67] A duplex was again formed, with the crystal structure revealing that the R_2 alkoxide was coordinated (Figure 7c). The authors note that an equilibrium existed between the duplex and the $[M_2\mathbf{L12}_2(H_2O)]^{4+}$ system, where a water molecule bridged the copper(II) centers (as crystallized). In the presence of a borate buffer at pH 9.35, an applied voltage initiated the coordination of the borate buffer to one of the copper(II) centers and, in turn, allowed for the electrocatalytic oxidation of water. Maayan and co-workers have established that the "dangling" $-OH$ groups were also involved in the water oxidation process, potentially acting as a proton acceptor to allow for the B–O bond cleavage which enables water oxidation. Ultimately, the helical structure of the system stabilizes the position of the two copper(II) centers and neighboring $-OH$ groups to allow for the electrocatalysis of water oxidation.

3. METAL IONS PROMOTING THE FORMATION OF EXTENDED OR "OPEN" STRUCTURES

In contrast to structural codons that promote extended "linear" conformations without metal ions, alteration of the substitution pattern of the heterocyclic rings can result in favorability for the folded conformation. Barboiu and Lehn reported a ligand series constituted from pyridine–(pyridine–pyrimidine)$_n$–dipyridine, with n = 1, 2, 4, 5, and 8 (Figure 8).[68] These coiled in acetonitrile solution to helices, which for

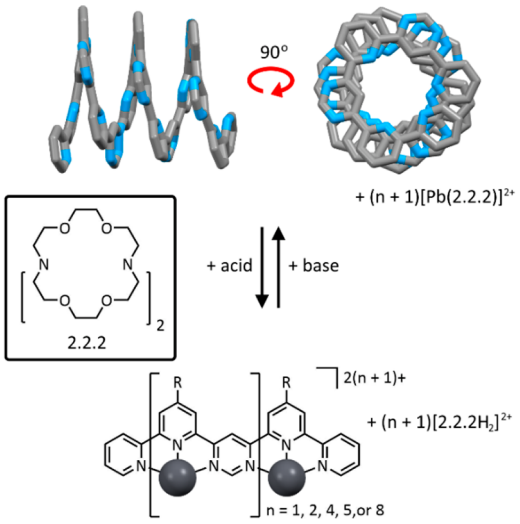

Figure 8. (Pyridyl)pyrimidine ligand system developed by Barboiu and Lehn,[68] which forms a helical coil without metal ions (shown as a model, for **L13**, n = 8), but extends into a linear conformation upon introduction of Pb(II). Switching between the two states was effected in the presence of the cryptand 2.2.2 through protonation/deprotonation of the cryptand. R = SPr, not shown in the molecular model of **L13**. Colors (model): carbon, gray; nitrogen, light blue; (chemical structure) lead, charcoal.

the longest ligand (**L13**, n = 8) had 3.2 turns and a length of approximately 11 Å. The introduction of Pb(II) (9 equiv for **L13**) prompted structural transformation into a linear extended secondary structure, $[Pb_9\mathbf{L13}]^{18+}$ (Figure 8), again assigned on the basis of 2D through-space NMR data. Modeling suggested this complex had a length of approximately 60 Å. In the presence of 9 equiv of the cryptand 2.2.2, the Pb(II) was sequestered from the complex forming $[Pb(2.2.2)]^{2+}$ species and reformation of the **L13** helix. Addition of acid ejected Pb(II) from the cryptand, which was protonated to $[2.2.2H_2]^{2+}$, reforming $[Pb_9\mathbf{L13}]^{18+}$, and this could, in turn, be reversed by introduction of base. Stadler and Lehn have also developed primary sequences which have two distinct domains, one that adopts an extended conformation (domain 1, constructed from pyridine, hydrazone and pyrimidine units) and another that coils (domain 2, repeating pyrimidine and hydrazone units with a pyridyl end cap), for example, **L14** (Figure 9).[69] Effecting the protonation/deprotonation of TREN with acid/base, the authors were able to introduce or extract Pb(II) from the system.

https://doi.org/10.1021/acsorginorgau.2c00021
ACS Org. Inorg. Au 2022, 2, 464–476

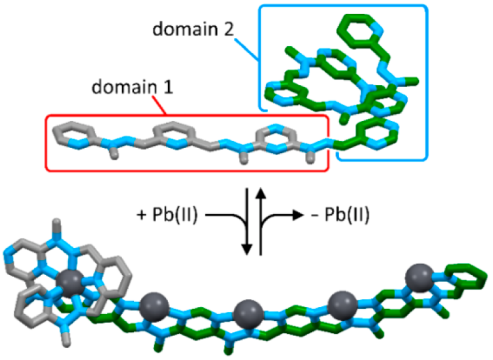

Figure 9. Ligand **L14** developed by Stadler and Lehn[69] that as a "free ligand" has an extended domain (domain 1) and a coiled domain (domain 2). Introduction of Pb(II) brought about conformational reversal of both of these domains. Pb(II) could be introduced or extracted using protonation/deprotonation of TREN also present in solution, in a similar fashion to other work by this group. Depictions are of molecular models; hydrogen atoms, ancillary ligands, and solubilizing elements have been omitted for clarity. Colors: carbon, gray (domain 1) or green (domain 2); nitrogen, light blue; lead, charcoal.

Coordination to the metal ion caused conformational reversal of the codons of the structure; hence, domain 1 coiled upon coordination, and domain 2 extended, and thus both secondary structural elements were reversed through metal coordination.

4. METAL IONS PROMOTING THE FORMATION OF TURNS

In protein/peptide chemistry, in addition to the α-helix and the extended strands that make up β-sheets, the third and final class of structural elements is "turns", which enable a reversal in direction of the primary sequence. An example has been reported by Shionoya and co-workers.[70]

The authors used [*n*]-repeating units of synthetic oxime-containing amino acids. The synthetic peptide chain analogues (Figure 10) were capped at the N-terminus with carboxybenzyl groups and at the C-terminus with either R = $-OCH_3$ (forming a terminal methoxy ester, *n* = 2, **L15**; *n* = 4, **L17**) or R = $-NH_2$ (forming a terminal amide, *n* = 2, **L16**). Note that these ligands were deprotonated at least to some degree during complexation, denoted here as L$-n$H. These ligands were combined with two palladium(II) sources: $Pd(OAc)_2$ (Pd(II) with a base) or $[Pd(CH_3CN)_4](BF_4)_2$ (Pd(II)). Structure was assigned in the resultant complexes through 2D NMR spectroscopic techniques and X-ray crystallography. With **L15**, this resulted in the formation of two different complexes (Figure 10). In the presence of acetate, both the amide and carbamate nitrogen atoms were deprotonated, and an N-terminal helix was formed with coordination through both of these atoms in addition to the two oxime nitrogen atoms: [Pd(**L15**$-$2H)]. The same experiment with **L16** gave a similar N-terminal [Pd(**L16**$-$2H)] complex as the major product but a minor (forming in a 3:7 ratio) product (also [Pd(**L16**$-$2H)]) which was a C-terminal helix, with coordination through the C-terminal amide nitrogen, the central amide nitrogen, and the two oxime nitrogen atoms.

With the BF_4^- salt and either ligand, the carbamate nitrogen was not deprotonated nor ligated to Pd(II). Coordination was instead through the two oxime nitrogen atoms, and the (deprotonated) amide nitrogen. In the X-ray crystal structure (obtained for **L16**) of this complex type, the final coordination

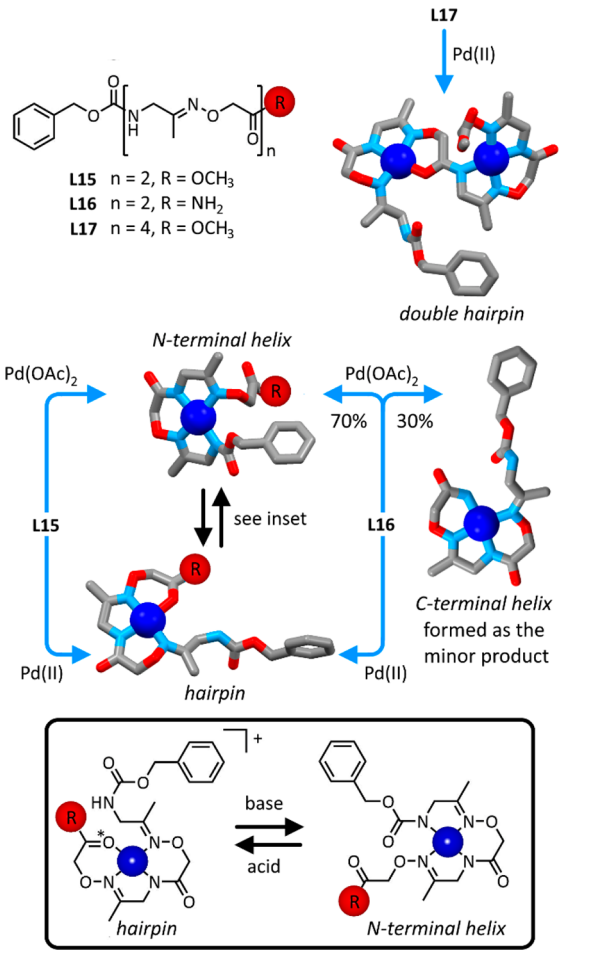

Figure 10. Ligands from repeating oxime-containing acids reported by Shionoya and co-workers.[70] Depending on the number of repeating units, the C-terminal capping unit (methoxy or amine) and the Pd(II) source (with a base (acetate) or without) they were able to access N-terminal and C-terminal helices and hairpin and double hairpin turns. Note, in the crystal structure and chemical structure for the hairpin, the C-terminal carbonyl group (*) is shown as coordinating; in solution, this site was occupied by solvent. All structures are from X-ray crystal structures, and structures from the N-terminal helix and hairpin complex are based upon those formed from ligands **L15** and **L16**, respectively. Colors: carbon, gray; nitrogen, light blue; oxygen, red; palladium, dark blue. Hydrogen atoms, counterions, and solvent molecules are omitted for clarity.

site of the Pd(II) ion was occupied by the carbonyl oxygen of the amide, but solution-phase data suggested that normally this site was occupied by solvent in the case of both ligands. Therefore, in these $[Pd(L-H)]^+$ complexes the palladium(II) metal ion therefore did not "cap" the sequence but enforced a hairpin turn. The group was able to switch between the N-terminal helix and the hairpin turn through the addition of acid or base (and the protonation or deprotonation of the carbamate nitrogen). They next turned to their tetra repeat ligand, **L17**. With a 1:2 ratio of **L17** to $[Pd(CH_3CN)_4](BF_4)_2$, a double hairpin complex was formed, $[Pd_2(\mathbf{L17}-3H)]^+$. The two hairpin conformations were bridged by a deprotonated amide group, and, as before with the BF_4^- salt, the carbamate nitrogen atom was not involved in coordination (Figure 10). The authors were able to employ the same base/acid stimuli to deprotonate this site and switch coordination modes, although the end result in this case is still a double hairpin, the resultant

https://doi.org/10.1021/acsorginorgau.2c00021
ACS Org. Inorg. Au 2022, 2, 464−476

[Pd_2(**L17**−4H)] complex was differently bridged and more flexible. Other dinuclear double-hairpin structures have also been reported by Setsune and co-workers with hexapyrrole dicarbaldehyde ligands, with Cu(II) and Ni(II),[71] with similar results also reported by Xie and co-workers.[72]

5. METAL IONS DISRUPTING THE FORMATION OF WELL-DEFINED SECONDARY STRUCTURES

There are also a few examples where molecules that adopt stable conformations have these conformations disrupted through coordination to metal ions: between folded and extended but ill-defined conformations.

This has been demonstrated in ferrocene-hinged structures, with aromatic substituents that prefer to fold into a closed state due to $\pi-\pi$ interactions. Incorporation of metal ion binding sites to the aromatic substituents has allowed coordination induced reversal of this folded state. Bosnich and co-workers synthesized a disubstituted ferrocene rotor (**L18**) with an *N*-methyl-3-pyridinium "arm" and a 2,2′-bipyridyl "arm" the latter of which was complexed to a neutral palladium dichloride unit.[73] The complex adopted a $\pi-\pi$ stacked, folded conformation. Upon addition of Ag(I) ions in the presence of pyridine, the chloride ligands were replaced with neutral pyridine ligands and the 1+/2+ charge repulsion between the "arms" resulted in an unfolded extended conformation. This conformation, unlike those discussed in section 3, is not well-defined, with rotation through a wide range of angles possible (excluding the folded state). Consecutive addition of Cl^- anions and Ag(I) ions provided a stimulus for folding/unfolding on command (Figure 11).

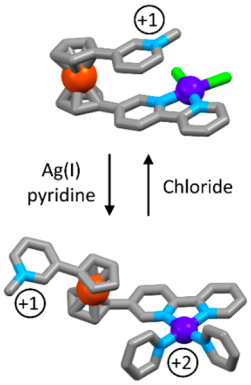

Figure 11. Bosnich and co-workers' early ferrocene-hinge-based rotor capable of folding and unfolding through reversible coordination of palladium ions effected by altering the coligands of the metal ion. X-ray crystal structures; hydrogen are atoms omitted for clarity. Colors: carbon, gray; nitrogen, light blue; iron, orange; palladium, dark blue. Hydrogen atoms, solvent, and counterions are omitted for clarity.

Later, Crowley and co-workers designed related systems with one or two 2,2′-bipyridyl "arms".[74] These folded in $CDCl_3$ solution, with density functional theory calculations indicating either a 3 kJ mol^{-1} preference or 6 kJ mol^{-1} preference for folded states over nonfolded states. These ferrocene-based ligands would adopt an unfolded state upon coordination of [Cu(I)(6,6′-dimesityl-2,2′-bipyridine)] units due to charge repulsion and steric interactions. Oxidation and reduction of the copper ions in the presence of terpyridine ligands provided a means of reversible switching between the folded and unfolded states. This concept was later applied to a larger "folding ruler" structure where two ferrocene rotor units joined three tiers together (**L19**, Figure 12). Folding was

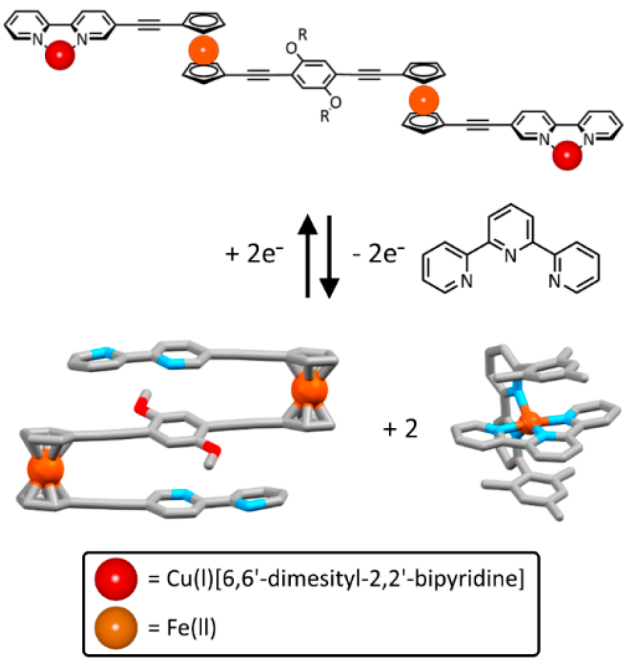

Figure 12. Crowley and co-workers' triple-tiered ferrocene-hinge based metallofoldamer. The ligand folds into a triple-tiered stack stabilized by $\pi-\pi$ interactions, but extends upon coordination of Cu(I)[6,6′-dimesityl-2,2′-bipyridine] units due to steric bulk. The process was fully reversible upon chemical or electrochemical oxidation and reduction of the copper ions in the presence of terpyridine. X-ray crystal structures; hydrogen atoms are omitted for clarity. Colors: carbon, gray; nitrogen, light blue; iron, orange; oxygen, red. Hydrogen atoms, solvent, and counterions are omitted for clarity.

favored by 10 kJ mol^{-1} (98% folded state). This allowed generation of greater length extension and contraction (~17 Å, to ~40 Å), providing support for the feasibility of even higher tiered systems.[75]

6. METAL IONS ALTERING HELIX PROPERTIES: STABILITY, HANDEDNESS, AND SINGLE TO DOUBLE HELIX CONVERSION

In the examples above of metal ions influencing the secondary structure of foldamers, the structural transformations upon introduction of the metal ion(s) are striking, resulting in conversion of structural types (to helices, extended structures, or turns). However, there are also important roles of metal ions in foldamers in which they do not enforce interchange between foldameric secondary structural types but instead bring about alterations to a preformed structural type, often a helix. The parameters that define a helix include the handedness, whether the helix is single- or double-stranded and, for double-stranded helices, whether the directionality of the strands is parallel or antiparallel. Metal ions have been employed with foldameric ligands to alter all of these properties. In this respect we include metal ions not only in their own right, but also in their ability to coordinate to ancillary ligands or interact with counterions/guests and thereby influence the structure.

6.2. Metal Ions Altering the Stability of Helices

The presence of metal ions has altered the stability of folded structures. Metal ions have been incorporated into many

https://doi.org/10.1021/acsorginorgau.2c00021
ACS Org. Inorg. Au 2022, 2, 464−476

synthetic DNA and DNA-like structures, through coordination to various groups.[76−79] By way of an example, Meggers and co-workers reported self-complementary glycol nucleic acid (GNA) sequences: 3′-CGHATHCG-2′ (**L20**), where H was a hydroxypyridone unit capable of coordinating to Cu(II) in a square planar fashion.[80] In combination with Cu(II) a [Cu_2**L20**$_2$] duplex forms (Figure 13). The coordination of

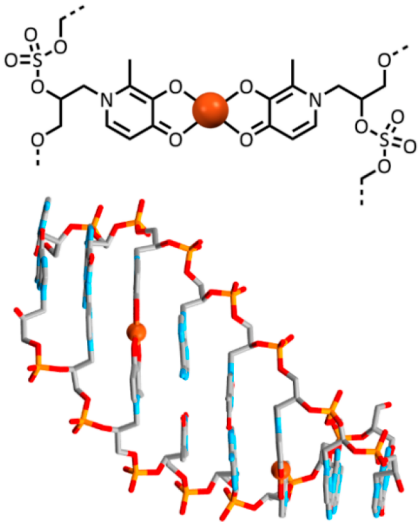

Figure 13. Top: Representation of the [Cu(hydroxypyridone)$_2$] units in the GNA duplex reported by Meggers and co-workers.[80] Bottom: X-ray crystal structure of the duplex, [Cu_2**L20**$_2$]. Colors: carbon, gray; copper, copper; nitrogen, light blue; oxygen, red; sulfur, orange. Hydrogen atoms omitted for clarity.

the Cu(II) greatly enhanced duplex stability: the melting temperature was 78 °C compared to 26 and 40 °C for nonmetal DNA and GNA variants. It seems clear, however, that care must be taken when introducing metal-binding sites: a study by Achim and co-workers introduced HQ units into peptide nucleic acid (PNA) ligands and found that steric considerations could reduce helix stability.[81]

6.3. Metal Ions Altering Handedness of Helices

Miyake and co-workers have achieved chirality inversion, with exchange of two water ligands at a Ni(II) center for nitrate.[82] Importantly, they have also coupled this inversion with a chiral ligand that has portions of a primary sequence with the capacity to coil into helical foldamers. The ligand (**L21**) was derived from *N*,*N*′-ethylenebis(*N*-methyl-(*S*)-alanine) (the metal-binding site), which was integrated into the ligand via condensation with amino acid-containing tails (Figure 14). On its own, **L21** had a small positive CD signal at 270 nm, indicating some preference for *P* helix formation. This was greatly amplified through the introduction of M(II) metal ions: Co(II), Ni(II), or Zn(II). Crystallization of the Zn(II) complex revealed a foldamer with two *P*-folded helices, and the coordination sphere of the Zn(II) metal occupied by the central C═O, N, N, C═O tetradentate site and two water molecules (Figure 14). The metal ion was in the Λ isomer, hence the [M**L21**]$^{2+}$ complex had an overall *P*Λ*P* isomeric identity. This isomeric form was enforced through hydrogen bonding between carbonyl oxygens and amide NH groups within the structure. Upon introduction of NO_3^-, the metal center transformed to a [M**L21** (NO_3)]$^+$ complex in the Δ isomer, with displacement of the two water ligands by nitrate

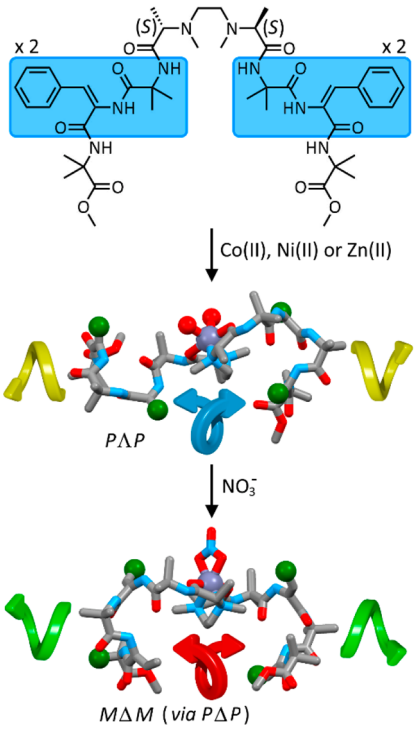

Figure 14. Chiral ligand (**L21**) reported by Miyake and co-workers[82] with a central carbonyl−amine−amine−carbonyl tetradentate site, with peptidic tails. Upon coordination to a metal ion, a *P*Λ*P* [M**L21** (H_2O)$_2$]$^{2+}$ complex was formed. Introduction of nitrate induced transformation to the *M*Δ*M* [M**L21** (NO_3)]$^+$ complex, with slow exchange of the helical tails from *P* to *M*. Depictions are from X-ray crystal structures, which were obtained for Zn(II), colors: carbon, gray; nitrogen, light blue; oxygen, red; zinc, metallic gray. Benzyl groups are shown as dark green spheres for clarity.

in bidentate mode. This resulted in the conversion of the tails to *M* folded helices (and hence the *M*Δ*M* isomer), which the authors attribute to stabilization by hydrophobic interactions, CH−π interactions, and hydrogen-bonding interactions. Interestingly, it was established that conversion from *P*Λ*P* to the *M*Δ*M* isomer was via the *P*Δ*P* isomer. Therefore, the metal ion altered its configuration upon nitrate coordination, prior to switching from *P* to *M* handedness in the helical tails. The same group has also managed to achieve chirality inversion in Pd(II) complexes through heating and/or microwave irradiation.[83]

Ag(I)-containing helices have also been reported by Cuerva and co-workers using poly-*ortho*-phenylene ethynylene ligands, with coordination between the metal ion and alkyne units in the ligand backbone.[84] With chiral sulfoxide termini, this resulted in an inversion switch (and higher conformational definition).[85]

6.4. Metal Ions Converting Single Helices to Double Helices

There have been examples reported in which the ligand adopts a single helix conformation in the absence of metal ion(s) but is converted to a double helix once a metal ion is introduced. An example of this has been reported by Jeong and co-workers,[86] with a ligand that consists of a central pyridine with 2,6-substitution with ethynyl linkers to two indolocarbazole units which were connected via additional alkynes to at one end a pyridine, and at the other, a 2-isopropyl alcohol group (**L22**). Relative to the central diethynylpyridine, the

https://doi.org/10.1021/acsorginorgau.2c00021
ACS Org. Inorg. Au 2022, 2, 464−476

indolocarbazole units could either be *syn* or *anti* in conformation (Figure 15). Both computations and crystallography confirmed *syn*−*syn*, the helical conformation, was preferred. The combination of **L22** with $[Pd(CH_3CN)_2Cl_2]$ in 2:2 ratio resulted in the slow formation of dinuclear double-stranded helix complexes, where two organic helices came together about two $[PdCl_2]$ units as shown by X-ray crystallography. However, crystallization from different solvent combinations gave two different structures. In the first, the two ligands of the double helix were both of the *syn* conformation while the other exhibited a *syn-anti* pairing.

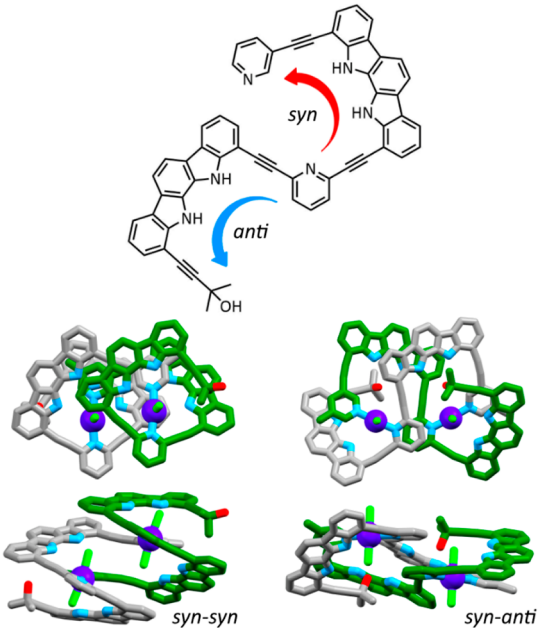

Figure 15. Top: Ligand **L22** developed by Jeong and co-workers, with one arm shown *syn* to the central pyridine and the other *anti*. In 2:2 combination with $Pd(II)Cl_2$, $[(PdCl_2)_2\mathbf{L22}_2]$ double-stranded foldamer complexes formed. Bottom: Two distinct isomeric complexes were obtained, with both ligands in each complex adopting either *syn*−*syn* or *syn*−*anti* conformation. Colors: carbon, gray or green; chloride, light green; nitrogen, light blue; oxygen, red; palladium, dark blue. Hydrogen atoms are omitted for clarity.

In both cases, the metal ions were each coordinated by a central pyridine of one ligand and the terminal pyridine of the other. The chloride ligands acted to stabilize the structures through hydrogen bonds to the NH moieties of the indolocarbazole groups. It was shown via variable temperature NMR studies that conversion from the *syn*−*anti* species to the *syn*−*syn* helicate in solution was possible by increasing the temperature, indicating that *syn*−*syn* was the entropically favored conformation while *syn*−*anti* was enthalpically favored.

Zhu and Liu and co-workers[30] reported triazole linked-phenanthroline ligands which adopted a helical conformation, due to $\pi-\pi$ interactions and hydrogen bonding between the hydrogen atoms of the triazole groups and nitrogen atoms of the phenanthroline groups. This helical conformation was inferred in solution through NMR spectroscopy, specifically by downfield shifts of hydrogen-bonding triazoles, and 2D through-space couplings. The X-ray crystal structure of the ligand revealed an internal diameter of 3.6 Å and a helical pitch of 3.5 Å (2.3 units per turn), and in the extended solid state the ligands formed oligomeric channels, through $\pi-\pi$ interactions, with significant space for incorporation of small guests. Upon copper ion complexation a double-stranded helix is formed with three Cu(I) and one Cu(II) ion coordinated by two intertwined ligands. The resulting structure has no space inside the helix. Moreover, the authors demonstrated the reversible interconversion between the hollow channels of the ligands extended solid state structure and the "closed" structure of the copper complex. The authors incorporated the hollow helical tubes into lipid bilayers and showed that ion transport through these channels was not only possible but could be reversibly switched off upon addition of copper ions.

6.5. Metal Ions Controlling Strand Directionality in Double-Stranded Helices

When a linear primary sequence has directionality, its incorporation into a double-stranded helical secondary structure can potentially give rise to different diastereoisomers dependent on the relative orientation of the strands, such as parallel or antiparallel arrangements (Figure 16).

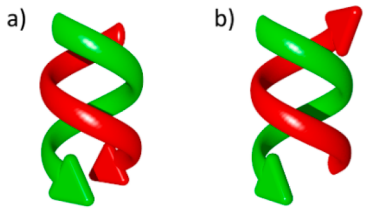

Figure 16. Relative orientation of directional sequences in double-stranded foldamers: (a) parallel and (b) antiparallel, both shown for left-handed helices.

Fujita and co-workers[87] explored control over this isomerism with a series of three octapeptides made up of alternating L- and D-amino acids with the two termini protected. Present in each octapeptide were six valine residues and two 3-pyridylanaline residues. It had previously been observed that alternating L- and D-alanine octapeptides form equilibrium mixtures of different isomeric double-stranded helices in solution, driven by hydrogen-bonding interactions following the patterns seen in β-sheet secondary structures: parallel and antiparallel arrangements. With the use of the dipyridyl-substituted ligands in 2:2 combination with $Zn(II)I_2$ to give $[(ZnI_2)_2(ligand)_2]$ complexes in 1:1 chloroform/acetone. In these complexes, control over relative strand directionality was achieved (Figure 17). For example, with **L23** which possessed pyridyl groups at positions R_3 and R_5, quantitative parallel orientation and the formation of the left-handed helix were achieved. This was driven through coordination to each of the Zn(II) metal ions by pyridyl groups at positions 3 and 7 on different strands, with the last two sites on the tetrahedral metal centers occupied by iodide ligands. In the case of **L24** and **L25** which had pyridyl groups at positions R_5 and R_7 or R_3 and R_7, respectively, two different antiparallel forms were exclusively accessed. In addition to granting control over directionality, coordination to Zn(II) provided much higher stability of the dimer under dilute conditions.

7. CONCLUSIONS AND FUTURE DIRECTIONS

The different roles that metal ions can play in promoting or otherwise altering the structure of defined foldameric molecules are now well understood and, depending on the design of the system, can be involved in various different ways

https://doi.org/10.1021/acsorginorgau.2c00021
ACS Org. Inorg. Au 2022, 2, 464−476

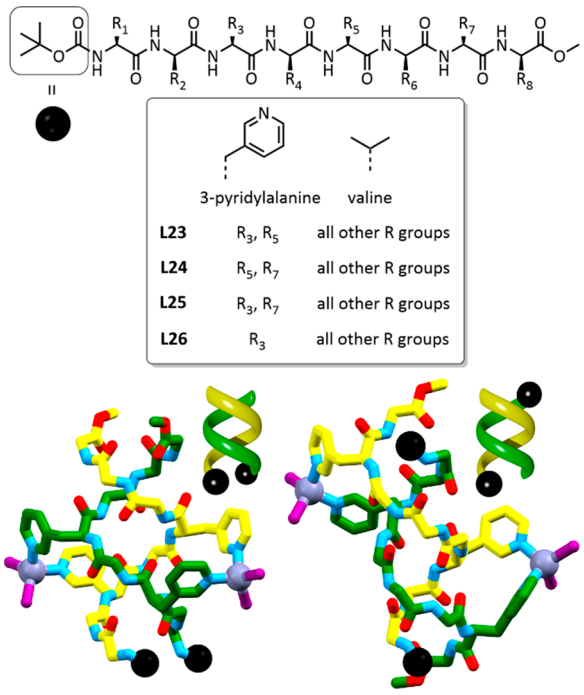

Figure 17. Top: General form for octapeptide ligands utilized by Fujita and co-workers for control over directionality in double-stranded helices. Inset: Identity of residues within each of the ligands. Bottom: Representations of the crystal structures of parallel helix $[(ZnI_2)_2\mathbf{L23}_2]$ and antiparallel helix $[(ZnI_2)_2\mathbf{L25}_2]$. Colors: carbon, green or yellow; iodide, magenta; nitrogen, light blue; oxygen, red; zinc, metallic gray. Hydrogen atoms are omitted for clarity, and Boc protecting groups are represented by black spheres.

at different hierarchical levels in the structures. Up to now, most of this involvement has been structural, but an enormous scope exists for the use of metal ions in foldamers to create functional molecules. Examples have emerged that point toward the directions and examples in which foldamers may one day fulfill applications outside of academic research, in industry and medicine.

Some of these examples rise from the capacity for coordination to a metal to alter the structure of the system: this has seen foldameric structures be utilized as metal ion sensors[88−90] and as a metal coordination stimulated actuator.[91] In the previously discussed example from Zhu and Liu and co-workers,[30] foldameric helices could be inserted into bilayers, and ion transport could be blocked by addition of Cu(II) which coordinated to the foldamers with a single- to double-stranded switch. In other cases, the coordination to the metal ion improves the characteristics of the foldamer, such as the Cu(II)-containing GNA duplex from Meggers and co-workers.[80]

Metal-containing molecules with defined conformations may also become useful for medicinal applications. The value of peptide-based therapeutics has been known for a considerable time,[92] while there is the capacity for metal ions to contribute to medicine in novel ways as, for example, antimicrobials.[93] Metallofoldamers may be able to contribute in these areas.[94,95] Additionally, metallofoldamers may also be able to replicate the behavior of metal-binding biopolymers, selectively binding specific metal ions. This has been demonstrated by the Maayan group with selective Zn(II) binding,[96] dual Cu(II)/Zn(II) binding,[97] and Cu(II) binding that can extract the metal ion from amyloid-β peptides, preventing the formation of reactive oxygen species that have been associated with Alzheimer's disease.[98]

Metal ions have long been of interest to chemists for their electronic character, their ability to switch oxidation states, and their reactivity. Examples are also beginning to arise where these facets give interesting character to foldameric molecules. Huc and co-workers recently reported polyaromatic amide helices that bind Cu(II) ions, which in the solid state form linear arrays and can transport electrons.[99] Another example is the Maayan peptoid-based double-stranded Cu(II) system with the capacity for electrocatalytic water oxidation.[67]

Lastly, the molecular environment may potentially be tuned to alter the character of the metal ions bound,[100] creating the possibility of metal ions within foldamers to have their reactivity and character tuned in the same fashion that nature has employed to such success in metalloenzymes. Together with a strong grasp over the roles that metal ions can play in foldamer structure, metallofoldamers should increasingly find applications as functional molecules, especially as emerging functions continue to develop.

AUTHOR INFORMATION

Corresponding Author

Dan Preston − *Research School of Chemistry, Australian National University, Canberra, ACT 2601, Australia;* orcid.org/0000-0002-1093-8153; Email: daniel.preston@anu.edu.au

Authors

Jess L. Algar − *Research School of Chemistry, Australian National University, Canberra, ACT 2601, Australia*

James A. Findlay − *Research School of Chemistry, Australian National University, Canberra, ACT 2601, Australia*

Complete contact information is available at: https://pubs.acs.org/10.1021/acsorginorgau.2c00021

Author Contributions

The manuscript was written through contributions of all authors. All authors have given approval to the final version of the manuscript. CRediT: **Jess Louise Algar** writing-original draft (equal), writing-review & editing (equal); **James Alan Findlay** writing-original draft (supporting), writing-review & editing (supporting); **Dan Preston** conceptualization (lead), writing-original draft (equal), writing-review & editing (equal).

Funding

DECRA Fellowship, ARC.

Notes

The authors declare no competing financial interest.

ACKNOWLEDGMENTS

D.P. thanks the Australian Research Council for a DECRA fellowship (DE200100421). J.L.A. thanks the Australian National University for a National University Scholarship. The authors thank the Australian National University for additional funding.

REFERENCES

(1) Chakrabarty, R.; Mukherjee, P. S.; Stang, P. J. Supramolecular coordination: self-assembly of finite two- and three-dimensional ensembles. *Chem. Rev.* **2011**, *111* (11), 6810−6918.

(2) Harris, K.; Fujita, D.; Fujita, M. Giant hollow MnL2n spherical complexes: structure, functionalisation and applications. *Chem. Commun.* **2013**, *49* (60), 6703−6712.
(3) Martín Díaz, A. E.; Lewis, J. E. M. Structural Flexibility in Metal-Organic Cages. *Front. Chem.* **2021**, *9*.
(4) Hill, D. J.; Mio, M. J.; Prince, R. B.; Hughes, T. S.; Moore, J. S. A Field Guide to Foldamers. *Chem. Rev.* **2001**, *101* (12), 3893−4012.
(5) Mazzier, D.; De, S.; Wicher, B.; Maurizot, V.; Huc, I. Parallel Homochiral and Anti-Parallel Heterochiral Hydrogen-Bonding Interfaces in Multi-Helical Abiotic Foldamers. *Angew. Chem., Int. Ed.* **2020**, *59* (4), 1606−1610.
(6) Hou, J.-L.; Shao, X.-B.; Chen, G.-J.; Zhou, Y.-X.; Jiang, X.-K.; Li, Z.-T. Hydrogen Bonded Oligohydrazide Foldamers and Their Recognition for Saccharides. *J. Am. Chem. Soc.* **2004**, *126* (39), 12386−12394.
(7) Borissov, A.; Lim, J. Y. C.; Brown, A.; Christensen, K. E.; Thompson, A. L.; Smith, M. D.; Beer, P. D. Neutral iodotriazole foldamers as tetradentate halogen bonding anion receptors. *Chem. Commun.* **2017**, *53* (16), 2483−2486.
(8) Massena, C. J.; Wageling, N. B.; Decato, D. A.; Martin Rodriguez, E.; Rose, A. M.; Berryman, O. B. A Halogen-Bond-Induced Triple Helicate Encapsulates Iodide. *Angew. Chem., Int. Ed.* **2016**, *55* (40), 12398−12402.
(9) Borissov, A.; Marques, I.; Lim, J. Y. C.; Félix, V.; Smith, M. D.; Beer, P. D. Anion Recognition in Water by Charge-Neutral Halogen and Chalcogen Bonding Foldamer Receptors. *J. Am. Chem. Soc.* **2019**, *141* (9), 4119−4129.
(10) Scott Lokey, R.; Iverson, B. L. Synthetic molecules that fold into a pleated secondary structure in solution. *Nature* **1995**, *375* (6529), 303−305.
(11) Sebaoun, L.; Kauffmann, B.; Delclos, T.; Maurizot, V.; Huc, I. Assessing Stabilization through $\pi-\pi$ Interactions in Aromatic Oligoamide β-Sheet Foldamers. *Org. Lett.* **2014**, *16* (9), 2326−2329.
(12) Bornhof, A.-B.; Bauzá, A.; Aster, A.; Pupier, M.; Frontera, A.; Vauthey, E.; Sakai, N.; Matile, S. Synergistic Anion−(π)n−π Catalysis on π-Stacked Foldamers. *J. Am. Chem. Soc.* **2018**, *140* (14), 4884−4892.
(13) Seoudi, R. S.; Del Borgo, M. P.; Kulkarni, K.; Perlmutter, P.; Aguilar, M.-I.; Mechler, A. Supramolecular self-assembly of 14-helical nanorods with tunable linear and dendritic hierarchical morphologies. *new J. Chem.* **2015**, *39* (5), 3280−3287.
(14) Hill, D. J.; Moore, J. S. Helicogenicity of solvents in the conformational equilibrium of oligo(m-phenylene ethynylene)s: Implications for foldamer research. *Proc. Nat. Acad. Sci.* **2002**, *99* (8), 5053−5057.
(15) Qi, T.; Maurizot, V.; Noguchi, H.; Charoenraks, T.; Kauffmann, B.; Takafuji, M.; Ihara, H.; Huc, I. Solvent dependence of helix stability in aromatic oligoamide foldamers. *Chem. Commun.* **2012**, *48* (51), 6337−6339.
(16) Hua, Y.; Flood, A. H. Flipping the switch on chloride concentrations with a light-active foldamer. *J. Am. Chem. Soc.* **2010**, *132* (37), 12838−12840.
(17) Hua, Y.; Liu, Y.; Chen, C. H.; Flood, A. H. Hydrophobic collapse of foldamer capsules drives picomolar-level chloride binding in aqueous acetonitrile solutions. *J. Am. Chem. Soc.* **2013**, *135* (38), 14401−14412.
(18) Wang, Y.; Bie, F.; Jiang, H. Controlling Binding Affinities for Anions by a Photoswitchable Foldamer. *Org. Lett.* **2010**, *12* (16), 3630−3633.
(19) Wu, B.; Jia, C.; Wang, X.; Li, S.; Huang, X.; Yang, X.-J. Chloride Coordination by Oligoureas: From Mononuclear Crescents to Dinuclear Foldamers. *Org. Lett.* **2012**, *14* (3), 684−687.
(20) Suk, J.-m.; Naidu, V. R.; Liu, X.; Lah, M. S.; Jeong, K.-S. A Foldamer-Based Chiroptical Molecular Switch That Displays Complete Inversion of the Helical Sense upon Anion Binding. *J. Am. Chem. Soc.* **2011**, *133* (35), 13938−13941.
(21) Saha, S.; Kauffmann, B.; Ferrand, Y.; Huc, I. Selective Encapsulation of Disaccharide Xylobiose by an Aromatic Foldamer Helical Capsule. *Angew. Chem., Int. Ed.* **2018**, *57* (41), 13542−13546.
(22) Prince, R. B.; Barnes, S. A.; Moore, J. S. Foldamer-Based Molecular Recognition. *J. Am. Chem. Soc.* **2000**, *122* (12), 2758−2762.
(23) Collie, G. W.; Bailly, R.; Pulka-Ziach, K.; Lombardo, C. M.; Mauran, L.; Taib-Maamar, N.; Dessolin, J.; Mackereth, C. D.; Guichard, G. Molecular Recognition within the Cavity of a Foldamer Helix Bundle: Encapsulation of Primary Alcohols in Aqueous Conditions. *J. Am. Chem. Soc.* **2017**, *139* (17), 6128−6137.
(24) Müller, M. M.; Windsor, M. A.; Pomerantz, W. C.; Gellman, S. H.; Hilvert, D. A Rationally Designed Aldolase Foldamer. *Angew. Chem., Int. Ed.* **2009**, *48* (5), 922−925.
(25) Maayan, G.; Ward, M. D.; Kirshenbaum, K. Folded biomimetic oligomers for enantioselective catalysis. *Proc. Nat. Acad. Sci.* **2009**, *106* (33), 13679−13684.
(26) Darapaneni, C. M.; Ghosh, P.; Ghosh, T.; Maayan, G. Unique β-Turn Peptoid Structures and Their Application as Asymmetric Catalysts. *Chem.—Eur. J.* **2020**, *26* (43), 9573−9579.
(27) Schettini, R.; Nardone, B.; De Riccardis, F.; Della Sala, G.; Izzo, I. Cyclopeptoids as Phase-Transfer Catalysts for the Enantioselective Synthesis of α-Amino Acids. *Eur. J. Org. Chem.* **2014**, *2014* (35), 7793−7797.
(28) Bécart, D.; Diemer, V.; Salaün, A.; Oiarbide, M.; Nelli, Y. R.; Kauffmann, B.; Fischer, L.; Palomo, C.; Guichard, G. Helical Oligourea Foldamers as Powerful Hydrogen Bonding Catalysts for Enantioselective C−C Bond-Forming Reactions. *J. Am. Chem. Soc.* **2017**, *139* (36), 12524−12532.
(29) Chen, F.; Shen, J.; Li, N.; Roy, A.; Ye, R.; Ren, C.; Zeng, H. Pyridine/Oxadiazole-Based Helical Foldamer Ion Channels with Exceptionally High K+/Na+ Selectivity. *Angew. Chem., Int. Ed.* **2020**, *59* (4), 1440−1444.
(30) Bai, D.; Yan, T.; Wang, S.; Wang, Y.; Fu, J.; Fang, X.; Zhu, J.; Liu, J. Reversible Ligand-Gated Ion Channel via Interconversion between Hollow Single Helix and Intertwined Double Helix. *Angew. Chem., Int. Ed.* **2020**, *59* (32), 13602−13607.
(31) Schettini, R.; Tosolini, M.; ur Rehman, J.; Shah, M. R.; Pierri, G.; Tedesco, C.; Della Sala, G.; De Riccardis, F.; Tecilla, P.; Izzo, I. Role of Lipophilicity in the Activity of Hexameric Cyclic Peptoid Ion Carriers. *Eur. J. Org. Chem.* **2021**, *2021* (3), 464−472.
(32) Mendez-Ardoy, A.; Markandeya, N.; Li, X.; Tsai, Y.-T.; Pecastaings, G.; Buffeteau, T.; Maurizot, V.; Muccioli, L.; Castet, F.; Huc, I.; et al. Multi-dimensional charge transport in supramolecular helical foldamer assemblies. *Chem. Sci.* **2017**, *8* (10), 7251−7257.
(33) Li, X.; Markandeya, N.; Jonusauskas, G.; McClenaghan, N. D.; Maurizot, V.; Denisov, S. A.; Huc, I. Photoinduced Electron Transfer and Hole Migration in Nanosized Helical Aromatic Oligoamide Foldamers. *J. Am. Chem. Soc.* **2016**, *138* (41), 13568−13578.
(34) Gellman, S. H. Foldamers: A Manifesto. *Acc. Chem. Res.* **1998**, *31* (4), 173−180.
(35) Zhang, D.-W.; Zhao, X.; Hou, J.-L.; Li, Z.-T. Aromatic Amide Foldamers: Structures, Properties, and Functions. *Chem. Rev.* **2012**, *112* (10), 5271−5316.
(36) Liu, C. Z.; Yan, M.; Wang, H.; Zhang, D. W.; Li, Z. T. Making Molecular and Macromolecular Helical Tubes: Covalent and Noncovalent Approaches. *ACS Omega* **2018**, *3* (5), 5165−5176.
(37) Huc, I. Aromatic Oligoamide Foldamers. *Eur. J. Org. Chem.* **2004**, *2004* (1), 17−29.
(38) Hartley, C. S. Folding of ortho-Phenylenes. *Acc. Chem. Res.* **2016**, *49* (4), 646−654.
(39) Goodman, C. M.; Choi, S.; Shandler, S.; DeGrado, W. F. Foldamers as versatile frameworks for the design and evolution of function. *Nat. Chem. Biol.* **2007**, *3* (5), 252−262.
(40) Maayan, G.; Albrecht, M. *Metallofoldamers: Supramolecular Architectures from Helicates to Biomimetics*; John Wiley and Sons, 2013.
(41) Maayan, G. Conformational Control in Metallofoldamers: Design, Synthesis and Structural Properties. *Eur. J. Org. Chem.* **2009**, *2009*, 5699−5710.
(42) Rao, S. R.; Schettler, S. L.; Horne, W. S. Metal-Binding Foldamers. *ChemPlusChem.* **2021**, *86* (1), 137−145.

https://doi.org/10.1021/acsorginorgau.2c00021
ACS Org. Inorg. Au 2022, 2, 464−476

(43) Nastri, F.; Chino, M.; Maglio, O.; Bhagi-Damodaran, A.; Lu, Y.; Lombardi, A. Design and engineering of artificial oxygen-activating metalloenzymes. *Chem. Soc. Rev.* **2016**, *45* (18), 5020−5054.
(44) Yu, F.; Cangelosi, V. M.; Zastrow, M. L.; Tegoni, M.; Plegaria, J. S.; Tebo, A. G.; Mocny, C. S.; Ruckthong, L.; Qayyum, H.; Pecoraro, V. L. Protein Design: Toward Functional Metalloenzymes. *Chem. Rev.* **2014**, *114* (7), 3495−3578.
(45) Prince, R. B.; Okada, T.; Moore, J. S. Controlling the secondary structure of nonbiological oligomers with solvophobic and coordination interactions. *Angew. Chem., Int. Ed.* **1999**, *38*, 233−236.
(46) Zhang, F.; Bai, S.; Yap, G. P. A.; Tarwade, V.; Fox, J. M. Abiotic Metallofoldamers as Electrochemically Responsive Molecules. *J. Am. Chem. Soc.* **2005**, *127* (30), 10590−10599.
(47) Akine, S.; Matsumoto, T.; Nabeshima, T. Spontaneous formation of a chiral supramolecular superhelix in the crystalline state using a single-stranded tetranuclear metallohelicate. *Chem. Commun.* **2008**, No. 38, 4604−4606.
(48) Akine, S.; Hotate, S.; Nabeshima, T. A Molecular Leverage for Helicity Control and Helix Inversion. *J. Am. Chem. Soc.* **2011**, *133* (35), 13868−13871.
(49) Akine, S.; Sairenji, S.; Taniguchi, T.; Nabeshima, T. Stepwise Helicity Inversions by Multisequential Metal Exchange. *J. Am. Chem. Soc.* **2013**, *135* (35), 12948−12951.
(50) Sairenji, S.; Akine, S.; Nabeshima, T. Lanthanide contraction for helicity fine-tuning and helix-winding control of single-helical metal complexes. *Dalton Trans.* **2016**, *45* (38), 14902−14906.
(51) Kawano, S.-i.; Narita, K.; Ikemoto, Y.; Sasaki, A.; Tanaka, K. Mesogenic discrete metallofoldamer for columnar liquid crystal. *Chem. Commun.* **2022**, *58* (20), 3274−3277.
(52) Baskin, M.; Zhu, H.; Qu, Z.-W.; Chill, J. H.; Grimme, S.; Maayan, G. Folding of unstructured peptoids and formation of hetero-bimetallic peptoid complexes upon side-chain-to-metal coordination. *Chem. Sci.* **2019**, *10* (2), 620−632.
(53) Leung, S. Y.-L.; Tam, A. Y.-Y.; Tao, C.-H.; Chow, H. S.; Yam, V. W.-W. Single-Turn Helix−Coil Strands Stabilized by Metal···Metal and $\pi-\pi$ Interactions of the Alkynylplatinum(II) Terpyridyl Moieties in meta-Phenylene Ethynylene Foldamers. *J. Am. Chem. Soc.* **2012**, *134* (2), 1047−1056.
(54) Chan, M. H.-Y.; Leung, S. Y.-L.; Yam, V. W.-W. Rational Design of Multi-Stimuli-Responsive Scaffolds: Synthesis of Luminescent Oligo(ethynylpyridine)-Containing Alkynylplatinum(II) Polypyridine Foldamers Stabilized by Pt···Pt Interactions. *J. Am. Chem. Soc.* **2019**, *141* (31), 12312−12321.
(55) Chan, M. H.-Y.; Ng, M.; Leung, S. Y.-L.; Lam, W. H.; Yam, V. W.-W. Synthesis of Luminescent Platinum(II) 2,6-Bis(N-dodecylbenzimidazol-2′-yl)pyridine Foldamers and Their Supramolecular Assembly and Metallogel Formation. *J. Am. Chem. Soc.* **2017**, *139* (25), 8639−8645.
(56) Preston, D. Discrete Self-Assembled Metallo-Foldamers with Heteroleptic Sequence Specificity. *Angew. Chem. Int. Ed.* **2021**, *60* (36), 20027−20035.
(57) Odriozola, I.; Kyritsakas, N.; Lehn, J.-M. Structural codons: linearity/helicity interconversion by pyridine/pyrimidine exchange in molecular strands. *Chem. Commun.* **2004**, No. 1, 62−63.
(58) Horeau, M.; Lautrette, G.; Wicher, B.; Blot, V.; Lebreton, J.; Pipelier, M.; Dubreuil, D.; Ferrand, Y.; Huc, I. Metal-Coordination-Assisted Folding and Guest Binding in Helical Aromatic Oligoamide Molecular Capsules. *Angew. Chem., Int. Ed.* **2017**, *56* (24), 6823−6827.
(59) Mateus, P.; Wicher, B.; Ferrand, Y.; Huc, I. Alkali and alkaline earth metal ion binding by a foldamer capsule: selective recognition of magnesium hydrate. *Chem. Commun.* **2017**, *53* (67), 9300−9303.
(60) Eerdun, C.; Hisanaga, S.; Setsune, J.-i. Single Helicates of Dipalladium(II) Hexapyrroles: Helicity Induction and Redox Tuning of Chiroptical Properties. *Angew. Chem. Int. Ed.* **2013**, *52* (3), 929−932.
(61) Eerdun, C.; Nguyen, T. H. T.; Okayama, T.; Hisanaga, S.; Setsune, J.-i. Conformational Changes and Redox Properties of Bimetallic Single Helicates of Hexapyrrole-α,ω-dicarbaldehydes. *Chem.—Eur. J.* **2019**, *25* (22), 5777−5786.
(62) Saito, S.; Furukawa, K.; Osuka, A. Fully π-Conjugated Helices from Oxidative Cleavage of meso-Aryl-Substituted Expanded Porphyrins. *J. Am. Chem. Soc.* **2010**, *132* (7), 2128−2129.
(63) Akine, S.; Nagumo, H.; Nabeshima, T. Hierarchical Helix of Helix in the Crystal: Formation of Variable-Pitch Helical π-Stacked Array of Single-Helical Dinuclear Metal Complexes. *Inorg. Chem.* **2012**, *51* (10), 5506−5508.
(64) Zhang, Y.; Thompson, A.; Rettig, S. J.; Dolphin, D. The Use of Dipyrromethene Ligands in Supramolecular Chemistry. *J. Am. Chem. Soc.* **1998**, *120* (51), 13537−13538.
(65) Ghosh, T.; Fridman, N.; Kosa, M.; Maayan, G. Self-Assembled Cyclic Structures from Copper(II) Peptoids. *Angew. Chem., Int. Ed.* **2018**, *57* (26), 7703−7708.
(66) Ghosh, P.; Fridman, N.; Maayan, G. From Distinct Metallopeptoids to Self-Assembled Supramolecular Architectures. *Chem.—Eur. J.* **2021**, *27* (2), 634−640.
(67) Ruan, G.; Ghosh, P.; Fridman, N.; Maayan, G. A Di-Copper-Peptoid in a Noninnocent Borate Buffer as a Fast Electrocatalyst for Homogeneous Water Oxidation with Low Overpotential. *J. Am. Chem. Soc.* **2021**, *143* (28), 10614−10623.
(68) Barboiu, M.; Lehn, J. M. Dynamic chemical devices: modulation of contraction/extension molecular motion by coupled-ion binding/pH change-induced structural switching. *Proc. Natl. Acad. Sci. U. S. A.* **2002**, *99* (8), 5201−5206.
(69) Stadler, A.-M.; Lehn, J.-M. P. Coupled Nanomechanical Motions: Metal-Ion-Effected, pH-Modulated, Simultaneous Extension/Contraction Motions of Double-Domain Helical/Linear Molecular Strands. *J. Am. Chem. Soc.* **2014**, *136* (9), 3400−3409.
(70) Tashiro, S.; Matsuoka, K.; Minoda, A.; Shionoya, M. Metallo-Foldamers with Backbone-Coordinative Oxime Peptides: Control of Secondary Structures. *Angew. Chem., Int. Ed.* **2012**, *51* (52), 13123−13127.
(71) Eerdun, C.; Nguyen, T. H. T.; Okayama, T.; Hisanaga, S.; Setsune, J.-i. Conformational Changes and Redox Properties of Bimetallic Single Helicates of Hexapyrrole-α,ω-dicarbaldehydes. *Chem.—Eur. J.* **2019**, *25* (22), 5777−5786.
(72) Zhang, K.; Savage, M.; Li, X.; Jiang, Y.; Ishida, M.; Mitsuno, K.; Karasawa, S.; Kato, T.; Zhu, W.; Yang, S.; et al. Rational syntheses of helical π-conjugated oligopyrrins with a bipyrrole linkage: geometry control of bis-copper(ii) coordination. *Chem. Commun.* **2016**, *52* (29), 5148−5151.
(73) Crowley, J. D.; Steele, I. M.; Bosnich, B. Protonmotive Force: Development of Electrostatic Drivers for Synthetic Molecular Motors. *Chem.—Eur. J.* **2006**, *12* (35), 8935−8951.
(74) Scottwell, S. Ø.; Elliott, A. B. S.; Shaffer, K. J.; Nafady, A.; McAdam, C. J.; Gordon, K. C.; Crowley, J. D. Chemically and electrochemically induced expansion and contraction of a ferrocene rotor. *Chem. Commun.* **2015**, *51* (38), 8161−8164.
(75) Scottwell, S. Ø.; Barnsley, J. E.; McAdam, C. J.; Gordon, K. C.; Crowley, J. D. A ferrocene based switchable molecular folding ruler. *Chem. Commun.* **2017**, *53* (54), 7628−7631.
(76) Takezawa, Y.; Müller, J.; Shionoya, M. Artificial DNA Base Pairing Mediated by Diverse Metal Ions. *Chem. Lett.* **2017**, *46* (5), 622−633.
(77) Popescu, D.-L.; Parolin, T. J.; Achim, C. Metal Incorporation in Modified PNA Duplexes. *J. Am. Chem. Soc.* **2003**, *125* (21), 6354−6355.
(78) Tanaka, K.; Clever, G. H.; Takezawa, Y.; Yamada, Y.; Kaul, C.; Shionoya, M.; Carell, T. Programmable self-assembly of metal ions inside artificial DNA duplexes. *Nat. Nanotechnol.* **2006**, *1* (3), 190−194.
(79) Engelhard, D. M.; Nowack, J.; Clever, G. H. Copper-Induced Topology Switching and Thrombin Inhibition with Telomeric DNA G-Quadruplexes. *Angew. Chem. Int. Ed.* **2017**, *56* (38), 11640−11644.
(80) Schlegel, M. K.; Essen, L.-O.; Meggers, E. Duplex Structure of a Minimal Nucleic Acid. *J. Am. Chem. Soc.* **2008**, *130* (26), 8158−8159.

https://doi.org/10.1021/acsorginorgau.2c00021
ACS Org. Inorg. Au 2022, 2, 464−476

(81) Ma, Z.; Olechnowicz, F.; Skorik, Y. A.; Achim, C. Metal Binding to Ligand-Containing Peptide Nucleic Acids. *Inorg. Chem.* **2011**, *50* (13), 6083−6092.
(82) Miyake, H.; Hikita, M.; Itazaki, M.; Nakazawa, H.; Sugimoto, H.; Tsukube, H. A Chemical Device That Exhibits Dual Mode Motions: Dynamic Coupling of Amide Coordination Isomerism and Metal-Centered Helicity Inversion in a Chiral Cobalt(II) Complex. *Chem.—Eur. J.* **2008**, *14* (18), 5393−5396.
(83) Miyake, H.; Ueda, M.; Murota, S.; Sugimoto, H.; Tsukube, H. Helicity inversion from left- to right-handed square planar Pd(ii) complexes: synthesis of a diastereomer pair from a single chiral ligand and their structure dynamism. *Chem. Commun.* **2012**, *48* (31), 3721−3723.
(84) Martín-Lasanta, A.; Álvarez de Cienfuegos, L.; Johnson, A.; Miguel, D.; Mota, A. J.; Orte, A.; Ruedas-Rama, M. J.; Ribagorda, M.; Cárdenas, D. J.; Carmen Carreño, M.; et al. Novel ortho-OPE metallofoldamers: binding-induced folding promoted by nucleating Ag(i)−alkyne interactions. *Chem. Sci.* **2014**, *5* (12), 4582−4591.
(85) Resa, S.; Miguel, D.; Guisán-Ceinos, S.; Mazzeo, G.; Choquesillo-Lazarte, D.; Abbate, S.; Crovetto, L.; Cárdenas, D. J.; Carreño, M. C.; Ribagorda, M.; et al. Sulfoxide-Induced Homochiral Folding of ortho-Phenylene Ethynylenes (o-OPEs) by Silver(I) Templating: Structure and Chiroptical Properties. *Chem.—Eur. J.* **2018**, *24* (11), 2653−2662.
(86) Jeon, H. G.; Lee, H. K.; Lee, S.; Jeong, K. S. Foldamer-based helicate displaying reversible switching between two distinct conformers. *Chem. Commun.* **2018**, *54* (45), 5740−5743.
(87) Sawada, T.; Iwasaki, W.; Yamagami, M.; Fujita, M. Parallel and antiparallel peptide double β-helices controlled by metal-induced folding and assembly. *Nat. Sci.* **2021**, *1* (1), No. e10008.
(88) Zhong, Z.; Zhao, Y. Cholate-Glutamic Acid Hybrid Foldamer and Its Fluorescent Detection of Zn2+. *Org. Lett.* **2007**, *9* (15), 2891−2894.
(89) Arunkumar, E.; Chithra, P.; Ajayaghosh, A. A Controlled Supramolecular Approach toward Cation-Specific Chemosensors: Alkaline Earth Metal Ion-Driven Exciton Signaling in Squaraine Tethered Podands. *J. Am. Chem. Soc.* **2004**, *126* (21), 6590−6598.
(90) Arunkumar, E.; Ajayaghosh, A.; Daub, J. Selective Calcium Ion Sensing with a Bichromophoric Squaraine Foldamer. *J. Am. Chem. Soc.* **2005**, *127* (9), 3156−3164.
(91) Schafmeister, C. E.; Belasco, L. G.; Brown, P. H. Observation of Contraction and Expansion in a Bis(peptide)-Based Mechanical Molecular Actuator. *Chem.—Eur. J.* **2008**, *14* (21), 6406−6412.
(92) Lau, J. L.; Dunn, M. K. Therapeutic peptides: Historical perspectives, current development trends, and future directions. *Bioorg. Med. Chem.* **2018**, *26* (10), 2700−2707.
(93) Frei, A.; Zuegg, J.; Elliott, A. G.; Baker, M.; Braese, S.; Brown, C.; Chen, F. G.; Dowson, C.; Dujardin, G.; Jung, N.; et al. Metal complexes as a promising source for new antibiotics. *Chem. Sci.* **2020**, *11* (10), 2627−2639.
(94) Pasco, M.; Dolain, C.; Guichard, G. Foldamers in Medicinal Chemistry. *Comprehensive Supramolecular Chemistry II* **2017**, 89−125.
(95) Montalvo, G. L.; Zhang, Y.; Young, T. M.; Costanzo, M. J.; Freeman, K. B.; Wang, J.; Clements, D. J.; Magavern, E.; Kavash, R. W.; Scott, R. W.; et al. De Novo Design of Self-Assembling Foldamers That Inhibit Heparin−Protein Interactions. *ACS Chem. Biol.* **2014**, *9* (4), 967−975.
(96) Ghosh, P.; Maayan, G. A rationally designed peptoid for the selective chelation of Zn2+ over Cu2+. *Chem. Sci.* **2020**, *11* (37), 10127−10134.
(97) Baskin, M.; Maayan, G. A rationally designed metal-binding helical peptoid for selective recognition processes. *Chem. Sci.* **2016**, *7* (4), 2809−2820.
(98) Behar, A. E.; Sabater, L.; Baskin, M.; Hureau, C.; Maayan, G. A Water-Soluble Peptoid Chelator that Can Remove Cu2+ from Amyloid-β Peptides and Stop the Formation of Reactive Oxygen Species Associated with Alzheimer's Disease. *Angew. Chem., Int. Ed.* **2021**, *60* (46), 24588−24597.
(99) Wang, J.; Wicher, B.; Méndez-Ardoy, A.; Li, X.; Pecastaings, G.; Buffeteau, T.; Bassani, D. M.; Maurizot, V.; Huc, I. Loading Linear Arrays of CuII Inside Aromatic Amide Helices. *Angew. Chem., Int. Ed.* **2021**, *60* (34), 18461−18466.
(100) Meunier, A.; Singleton, M. L.; Kauffmann, B.; Granier, T.; Lautrette, G.; Ferrand, Y.; Huc, I. Aromatic foldamers as scaffolds for metal second coordination sphere design. *Chem. Sci.* **2020**, *11* (44), 12178−12186.

https://doi.org/10.1021/acsorginorgau.2c00021
ACS Org. Inorg. Au 2022, 2, 464−476